Separation Science and Technology
Publication details, including instructions for authors and subscription information:
http://www.informaworld.com/smpp/title~content=t713708471

Equilibrium Adsorption Data from Breakthrough Curves with Variable Velocity and Pressure

F. Foeth[a]; H. Bosch[a]; A. Sjöstrand[b]; G. Aly[b]; T. Reith[a]
[a] FACULTY OF CHEMICAL ENGINEERING, UNIVERSITY OF TWENTE, AE ENSCHEDE, THE NETHERLANDS [b] DEPARTMENT OF CHEMICAL ENGINEERING, UNIVERSITY OF LUND, LUND, SWEDEN

To cite this Article Foeth, F. , Bosch, H. , Sjöstrand, A. , Aly, G. and Reith, T.(1996) 'Equilibrium Adsorption Data from Breakthrough Curves with Variable Velocity and Pressure', Separation Science and Technology, 31: 1, 21 — 38
To link to this Article: DOI: 10.1080/01496399608000678
URL: http://dx.doi.org/10.1080/01496399608000678

SEPARATION SCIENCE AND TECHNOLOGY, **31**(1), pp. 21–38, 1996

Equilibrium Adsorption Data from Breakthrough Curves with Variable Velocity and Pressure

F. FOETH and H. BOSCH
FACULTY OF CHEMICAL ENGINEERING
UNIVERSITY OF TWENTE
P.O. BOX 217, 7500 AE ENSCHEDE, THE NETHERLANDS

A. SJÖSTRAND and G. ALY
DEPARTMENT OF CHEMICAL ENGINEERING
UNIVERSITY OF LUND
P.O. BOX 124, S221 00 LUND, SWEDEN

T. REITH
FACULTY OF CHEMICAL ENGINEERING
UNIVERSITY OF TWENTE
P.O. BOX 217, 7500 AE ENSCHEDE, THE NETHERLANDS

ABSTRACT

In the framework of modeling PSA processes, column dynamics for the adsorption of mixtures of helium and carbon dioxide on activated carbon has been investigated under conditions where both flow rate and column pressure vary due to adsorption. A model has been developed based on the usual approximations of local equilibrium and isothermal conditions but allowing for changes in flow rate as well as column pressure. Experimental breakthrough curves were measured up to 27 kPa, corresponding to 20 mol% carbon dioxide. Good agreement between model and experimental curves was obtained up to 6 kPa and fair agreement up to 27 kPa carbon dioxide partial pressure. Adsorption isotherm data, required in the model calculations, have been obtained from these experimental step responses. These results are in good agreement with experimental equilibrium adsorption data obtained from both a static volumetric method and a gravimetric method.

INTRODUCTION

In the framework of modeling gas separation processes by dynamic methods such as (rapid) pressure swing adsorption (PSA), the column dynamics of the feed step have been studied. The prediction of the shape of a breakthrough curve is an essential step in the design of PSA columns. Adequate models should provide this information, thereby avoiding the tedious acquisition of experimental data.

Existing models distinguish between adsorption equilibrium and mass transfer limitation. The latter can be due to film resistance or resistance in the macro- or micropores. These resistances can be avoided in laboratory-scale equipment used for experimental verification by the use of small particles and low flow rates (1). Only in these experiments can isothermal conditions be ensured.

In models by Chihara and Suzuki (2), Carter and Wyszynski (3), and Yang et al. (4), the linear driving force approximation is used to describe the rate of mass transfer into the particles. The latter authors show that both a local equilibrium and a linear driving force model can adequately describe a full PSA cycle for the separation of H_2 and CH_4.

Equilibrium models, neglecting mass transfer limitations, which describe the feed step of a PSA cycle are based on the work of Shandelman and Mitchell (5) who applied such a model to dilute systems, using a linear adsorption isotherms and a constant velocity. Chan et al. (6) and Knaebel and Hill (7) extended this model to binary mixtures in which both components are adsorbed, while Nataraj and Wankat (8) extended this model to multicomponent mixtures.

The condition of linearity of the adsorption isotherm was relaxed by Flores Fernandez and Kenney (9), Yang et al. (4), Doong and Yang (10), Underwood (11), Lu et al. (12), Bossy et al. (13), Suh and Wankat (14) and Kayser and Knaebel (15). In the latter two publications the authors solved their set of partial differential equations (PDEs) analytically, whereas the others used numerical techniques.

All models discussed so far have the following assumptions in common:

- Ideal gas law
- Constant column pressure
- No pressure drop over the column
- No radial velocity and concentration gradients
- No axial dispersion
- Isothermal conditions

Laboratory-scale equipment used for verification purposes of a PSA feed step often have limited flow rates in which case dispersion has to be

taken into account. A system of PDEs including second-order terms, which are necessary to describe dispersion, has the additional advantage that it can be solved more easily numerically. LeVan and Vermeulen (16) and Foeth et al. (17) did this for nonlinear adsorption isotherms at constant pressure.

So far only limited attention has been paid to the flow resistances in the auxiliary devices of experimental (often laboratory-scale) equipment in general, such as detectors or valves in the product line. Baron et al. (18) introduced flow resistances of the valves in the feed line of an RPSA column. Kayser and Knaebel (19) varied the pressure during the feed step by making it dependent on the accumulation in the bed. Kumar (20) incorporated a valve equation in the blowdown step of a PSA process. Chou and Huang (21) incorporated the same valve equation in a two-bed air separation PSA process.

The main objectives of the present work are:

- To develop a mathematical model which describes step responses of a packed bed adsorber to changes in feed concentrations at conditions of varying pressure and velocity
- To calculate the equilibrium adsorption data needed in this model from the experimental breakthrough curves

To achieve these goals not only nonlinear adsorption and axial dispersion are taken into account, but also variable column pressure due to resistances in the auxiliary devices of our small-scale laboratory equipment.

EXPERIMENTAL

The main part of the experimental set-up (see Fig. 1) for the measurement of breakthrough curves was a modified gas chromatograph (Varian, type 3400) fitted with a thermal conductivity detector (TCD). In the oven a packed column was placed (the characteristics are given in Table 1). The column was packed with an activated carbon, type RB1 (Norit) having the properties displayed in Table 2.* The gases used were carbon dioxide (Hoekloos, 99.998% pure) and helium (Union Carbide, 99.999% pure); both were used without further purification.

Equilibrium adsorption isotherm data were obtained with a Carlo Erba Sorptomatic 1900, which employes a standard static volumetric technique, and with a thermobalance (HIDEN Analytical Ltd., IGA).

The feed, consisting of helium and carbon dioxide, was composed by means of mass flow controllers (Brooks, model 5850E). The mass flow

* The particle characteristics were supplied by Norit.

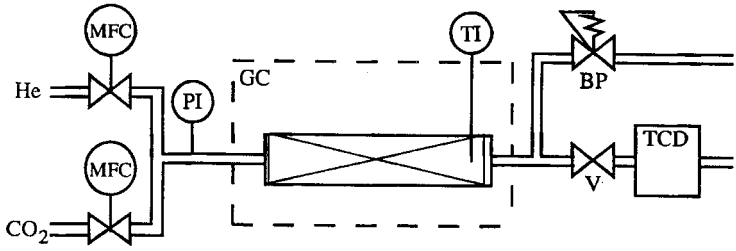

FIG. 1 The experimental set-up. MFC, mass flow controller; GC, oven of a gas chromatograph; BP, backpressure; V, valve; TCD, thermal conductivity detector; TI, thermocouple; PI, pressure transmitter.

controllers were calibrated by the use of a SAGA digital flow calibrator (Ion Service Ltd.).

The temperature difference between the exit of the column and the GC oven was monitored with a chromel-alumel thermocouple with a shell diameter of 1 mm. It was inserted 17 mm into the bed from the exit along the axis of the bed. The pressure at the inlet of the GC was monitored at regular time intervals using a digital pressure meter (J&W Scientific Inc., model 220-2062). The pressure drop over the auxilary devices was calibrated as a function of the total pressure, the mole fraction, and the flow rate.

At the start of an experiment a carbon dioxide flow was added to a constant mass flow of helium. The calibration of the TCD was carried out accordingly. Preceding the experiments, the column was conditioned at 200°C while purging with pure helium. After each run the column was reconditioned at 145°C for at least 1 hour.

Breakthrough measurements were performed at temperatures of 40 and 60°C, a total column pressure of 120–130 kPa, feed concentrations of 2–20

TABLE 1
Characteristics of the Adsorption Column

Weight of adsorbent	16.2 g
Length of the fixed bed	0.147 m
Internal column diameter	16.8 mm
Hydrodynamic particle radius	0.74 mm
External void fraction	0.37
Solid bulk density	497 kg/m^3

TABLE 2
Characteristics of Activated Carbon Type RB1

Total pore volume	0.728×10^{-3} m³/kg
Particle density	792 kg/m³
Internal void fraction	0.577
Particle shape	Cylindrical
Diameter	1.0 mm
Average length	2.16 mm

mol% carbon dioxide, and an interstitial gas velocity in the column of about 10 mm/s. The experiments were performed twice to check the reproducibility.

We also measured the effective molecular diffusivity in the activated carbon particles using a chromatographic method as described in Ref. 22. The resulting value for D_{eff} was approximately 1×10^{-7} m²/s at 40°C.

MODELING OF BREAKTHROUGH CURVES

A model has been developed which allows for changes in flow rate as well as column pressure. The change in column pressure, p, due to the pressure drop over the auxiliary devices was calculated as a calibrated function of the exit molar flow rate, ϕ_e, according to

$$p - p_{ambient} = (k_1 + k_2 y_e)\phi_e \tag{1}$$

An equilibrium model in which instant local equilibrium exists between the bulk of the fluid and the adsorbed phase is assumed. The combined effect of all dispersion mechanisms is lumped as a single effective axial dispersion coefficient calculated by means of the equations discussed by Wicke (23), using the modification by Langer et al. (24) for small particle sizes. Further assumptions are:

- The pressure drop over the column is negligible, since it is in the order of 10 Pa as estimated from the Ergun equation (25)
- The amount of helium adsorbed is negligible
- The Langmuir model is applicable for carbon dioxide adsorption:

$$q = \frac{q_{mono} B p y}{1 + B p y} \tag{2}$$

Under these conditions the mass balance equation for an adsorbable component is

$$\frac{\partial P y_i}{\partial \tau} + \frac{1-\epsilon}{\epsilon}\frac{\partial Q_i}{\partial \tau} = P\left(-\frac{\partial U y_i}{\partial z} + \frac{1}{\mathrm{Pe_m}}\frac{\partial^2 y_i}{\partial z^2}\right) \tag{3}$$

For a nonadsorbing component the second term of the left-hand side of Eq. (3) is omitted. For a binary mixture of carbon dioxide and nonadsorbing helium, summation of the relevant mass balance equations leads to

$$\frac{\partial P}{\partial \tau} + \frac{1-\epsilon}{\epsilon}\frac{\partial Q_{\mathrm{CO_2}}}{\partial \tau} = -P\frac{\partial U}{\partial z} \tag{4}$$

This equation describes the changes in gas velocity encountered in the column due to both the changes in pressure and the changes in the amount of locally adsorbed carbon dioxide.

The Dankwerts boundary conditions for this problem are

$$U\mathrm{Pe_m}(y_f - y) = -\partial y/\partial z, \qquad z = 0,\ t > 0 \tag{5a}$$

$$\partial y/\partial z = 0, \qquad z = 1,\ t > 0 \tag{5b}$$

and the remaining boundary condition is

$$UP = 1, \qquad z = 0,\ t > 0 \tag{5c}$$

The initial conditions are

$$y = 0, \qquad 0 \le z \le L,\ t = 0 \tag{6a}$$

$$UP = 1 - y_f, \qquad 0 \le z \le L,\ t = 0 \tag{6b}$$

The system of equations consisting of Eqs. (1)–(6) was solved by the use of an implementation of the numerical method of lines similar to that proposed by Schiesser (26). Prior to integration in time the derivatives in the z-direction were evaluated by means of finite difference library routines from DSS/2 (26). Thus the PDEs were converted to systems of ordinary differential equations (ODEs). Integration in time of the resulting stiff system of algebraic equations and ODEs was accomplished by employing LSODI (27). The solutions could only be obtained after implementing a differentiable sigmoid rise in the feed mole fraction, y_f, from zero to its proper value. This change took place in approximately 0.001% of the average residence time of the front.

RESULTS AND DISCUSSION

Column Pressure and Temperature

The column pressure and the temperature rise of the active carbon bed (measured 17 mm before the exit) have been monitored; typical results

are shown in Fig. 2. The temperature rise can be neglected except perhaps at the highest concentration of 20 mol%, where the maximum temperature rise is 1.5°C. The temperature front coincides with the concentration front, and the pressure rise coincides with the breakthrough.

Figure 2 also shows a significant increase in column pressure of 7 kPa during the breakthrough of carbon dioxide at the highest feed concentration of 20 mol%. The pressure rise is due to the increasing contribution of carbon dioxide to the total flow. This increase in flow resulted in an increase in pressure drop over the measuring devices located after the adsorption column. This effect was incorporated in the mathematical model, see Eq. (1). The rise can already be observed at the lowest concentration of 2 mol%. The highest pressure rise observed was 7 kPa.

Step Responses

Breakthrough curves in real time at feed concentrations of 5 to 20 mol% are given in Fig. 3. The result for 2 mol% in real time is presented in Fig. 6, which will be discussed at a later stage. The reproducibility of all experiments is good. The general pattern—shorter residence times and steeper curves at higher feed partial pressures—follows well-known theory, see, e.g., Ref. 28.

The shape of the breakthrough curves shown in Figs. 3 and 6 are influenced by various factors:

- A Langmuir, or similarly shaped, nonlinear isotherm steepens the concentration front, as lower concentrations travel slower than higher concentrations.

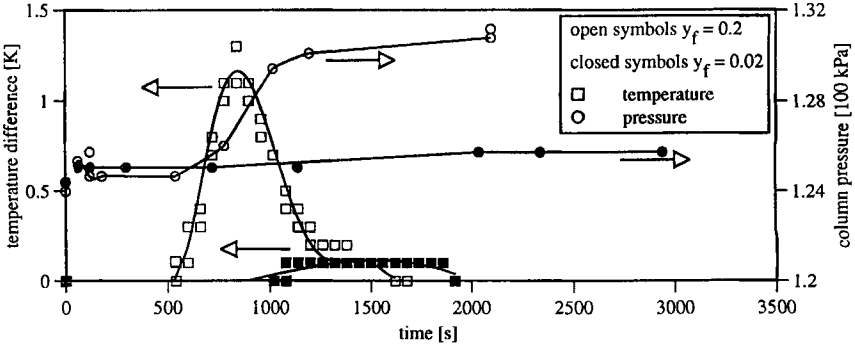

FIG. 2 Typical temperature and pressure measurement results at 60°C.

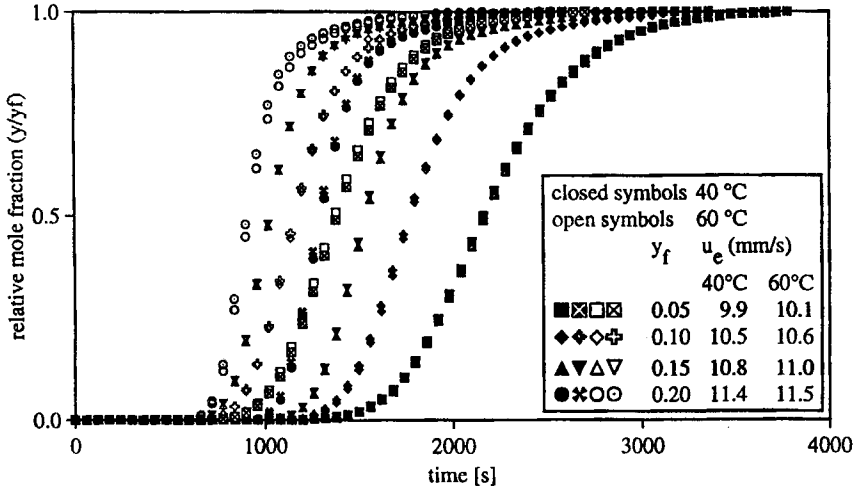

FIG. 3 Results of carbon dioxide breakthrough experiments at 40 and 60°C.

- The gas phase velocity rises when the front passes, thus high concentrations move more quickly than lower concentrations and the front steepens.
- The shapes of the curves are also influenced by the slight difference in axial dispersion in the various experiments; the larger the Péclet number, a measure for the amount of axial dispersion, the steeper the curve.
- The pressure rises during the passing of the front due to the auxiliary devices after the column. Because of the resulting rise in partial pressure, the maximum adsorption capacity of the packing becomes higher everywhere in the bed. This causes extra gas phase depletion along the length of the column which elongates the front.

Calculation of the Isotherms

The required amount adsorbed, q, is related to the holdup, which can be calculated from the experimental breakthrough curves by the use of the material balance:

$$q = \frac{\int_0^\infty (\phi_f y_f - \phi_e y_e)dt - \epsilon_t AL \frac{p_\infty}{RT} y_f}{W} \tag{7}$$

When evaluating the above integral, one has to take into account that

both the column pressure and the exit velocity vary during breakthrough. The exit flow rate was calculated by means of Eq. (1).

The isotherm points calculated (■, ●) above 5 kPa agree reasonably well with the equilibrium data obtained by both the static volumetric method and the gravimetric method, as can be seen in Fig. 4. At 40°C the volumetric and breakthrough data are in good agreement. The slightly scattered gravimetric data show a lower amount adsorbed, the difference is in the order of 8%. At 60°C the volumetric data agree well with the breakthrough data at high carbon dioxide partial pressures while at lower partial pressures the volumetric data agree well with the gravimetric data, which again are about 8% lower than the breakthrough data. The latter were fitted to the Langmuir adsorption isotherm model, see Eq. (2). The resulting parameter values are

$$\text{at } 40°\text{C: } q_{\text{mono}} = 1.90 \text{ mol/kg}, B = 2.43 \times 10^{-5} \text{ Pa}^{-1}$$

$$\text{at } 60°\text{C: } q_{\text{mono}} = 1.65 \text{ mol/kg}, B = 1.60 \times 10^{-5} \text{ Pa}^{-1}$$

These parameter values are used in the numerical simulation described in the next section.

The reference experiments were performed on different samples which were limited in size. Furthermore, the breakthrough measurements were

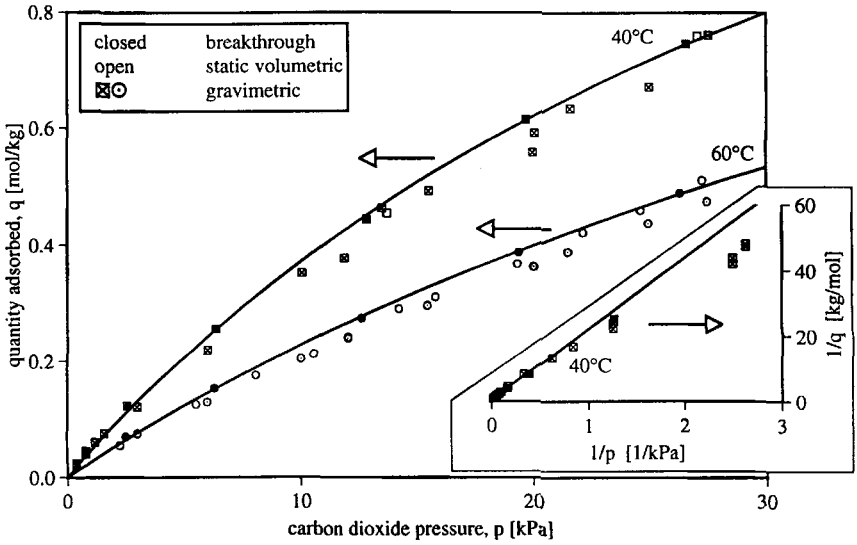

FIG. 4 Carbon dioxide adsorption isotherms on activated carbon. The inset shows the deviation from the linearized Langmuir isotherm at low pressures.

performed in a different environment than the volumetric and the gravimetric measurements because helium was present. Both these error sources may explain the differences between the results of the various techniques. Taking this into account, the breakthrough results agree favorably with the reference results.

The inset in Fig. 4 shows the reciprocal of both axes. In such a graph the Langmuir isotherm converts to a straight line. It is clear that at lower pressures more is adsorbed than is predicted by the Langmuir isotherm. This phenomenon is probably due to the heterogeneous nature of activated carbon surfaces.

Simulation Results

Both experimental data and simulation results for the concentrations of 5 mol% and higher are plotted in Fig. 5. There is good agreement between experiments and simulations. However, some deviation occurs at the highest concentrations (15 and 20 mol%). All the experimental and corresponding calculated breakthrough curves show average breakthrough times which differ by less than 1%. This good agreement indicates that the calculated isotherms are accurate for this application.

Temperature effects are unable to account for the differences between model and experiment. Temperature gradients in particles and transfer to and from the gas phase do not play a part, as the Péclet number for heat transfer that is based on the particle diameter is small (Pe_{hp} is in the order of 0.06) (29). Second, as temperature and concentration fronts coincide, the actual quantities adsorbed as a function of the local partial pressures do not follow the isotherm at the wall temperature, even in the absence of mass transfer limitation. Therefore the apparent isotherm would be curved more steeply at lower concentrations, which would yield a breakthrough curve of which the first part rises more steeply. This was not observed.

Mass transfer resistance probably accounts for the discrepancy between model and experiment at feed mole fractions larger than 5%. A test method is derived in the Appendix to indicate the influence of mass transfer limitation on the uptake of isothermal spherical particles:

$$\frac{\Delta q}{q_R} = \frac{\rho_s R^2}{15 q_R \mathbf{D}_{eff} c} \left(\frac{dq_R}{dy}\right)^2 \frac{\partial y_R}{\partial t} \tag{8}$$

where R is the radius of the particle, q_R is the amount adsorbed at the particle surface, Δq is the difference between the uptake at the particle surface and the average uptake, and y_R is the mole fraction in the bulk of the fluid. For the feed concentrations up to 5 mol%, $\Delta q/q_R$ ranged from 2–6% while for the higher feed concentrations the $\Delta q/q_R$ range was

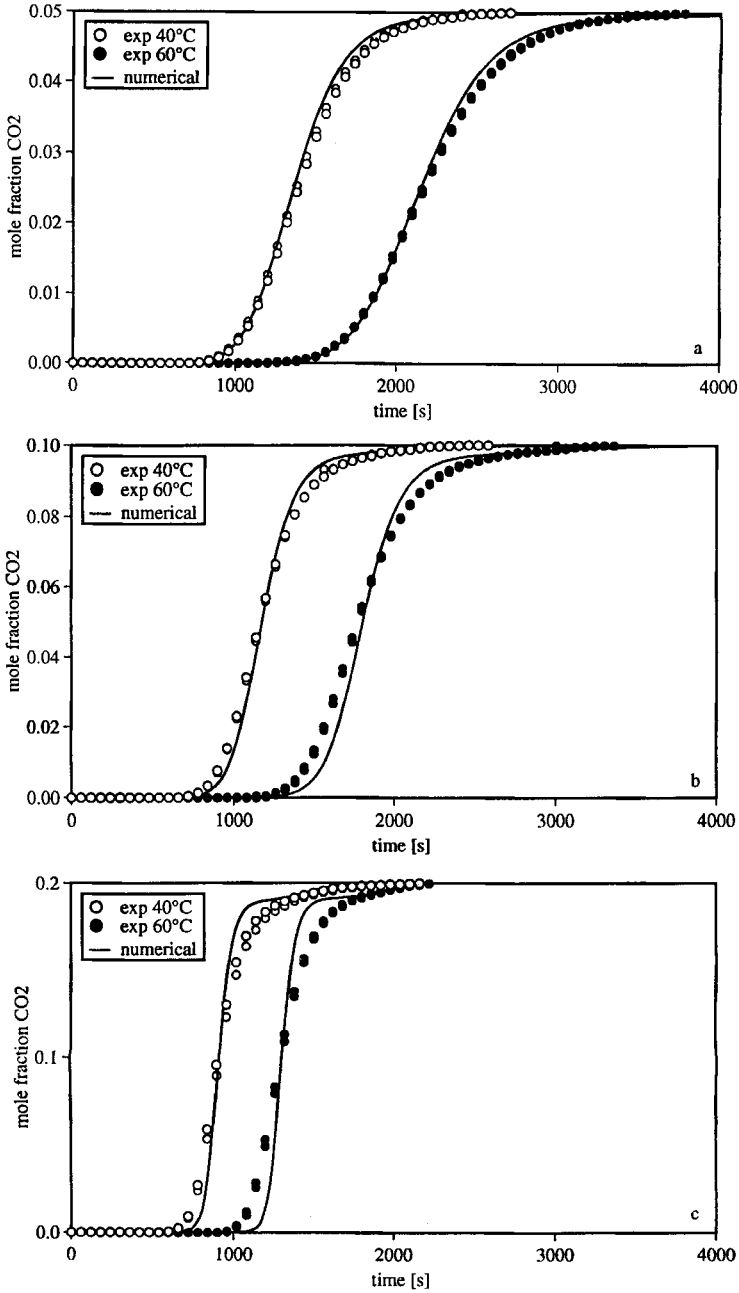

FIG. 5 Experimental and simulation results for feed concentrations of 5 mol% (a), 10 mol% (b), and 20 mol% (c).

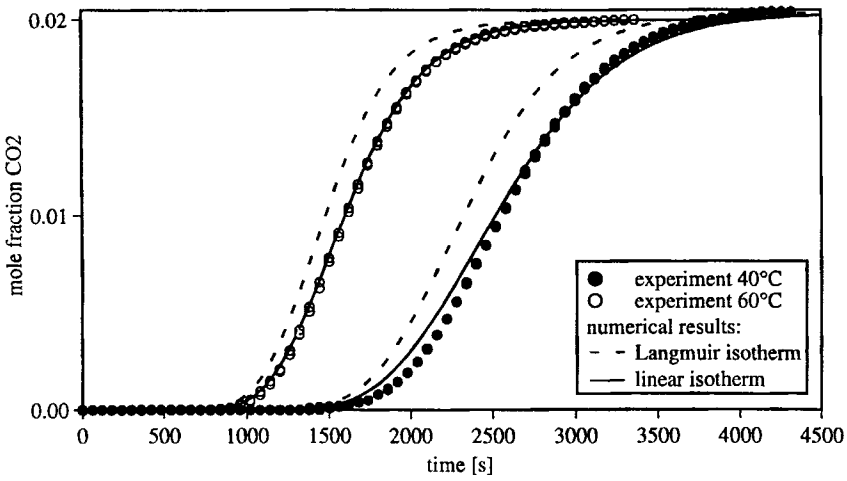

FIG. 6 Experimental and numerical results for a feed concentration of 2 mol%.

7–12%. This indicates that mass transfer limitation is more important in the 10–20% concentration range.

At the lowest feed concentration of 2 mol% a distinct deviation exists between the experimental residence times and those calculated from the Langmuir adsorption isotherms, as can be seen in Fig. 6. This is caused by the deviation from experimental data by the Langmuir isotherm; below 3 kPa adsorption data calculated from the fitted Langmuir isotherm are significantly below the experimental data shown in Fig. 4. When employing a linear isotherm through the data points below 3 kPa, good agreement between simulation and experiment was achieved, and there is a clear improvement over the result with the Langmuir isotherm. The use of one simple isotherm equation for the whole partial pressure range results in an underestimate of the initial slope, thus causing an underestimate in the residence time. This can be observed only in breakthrough curves at low mole fractions. At higher concentrations the deviations from the start of the isotherm are less important. The influence of the initial part of the isotherm is limited to a small and progressively smaller delay in the appearance of the breakthrough front.

CONCLUSIONS

Breakthrough curves of carbon dioxide through an activated carbon adsorption bed at conditions of variable flow rate and changing pressure

were calculated from known isotherm data and known flow resistances of the auxiliary devices.

Reliable equilibrium adsorption data were obtained from step response experiments at partial pressures above 4 kPa, provided the change in column pressure is taken into account.

The adsorption equilibrium model used in the simulation needs to be accurate in the initial part of the adsorption isotherm, as both the calculated residence time and the shape of the breakthrough curve are very sensitive to the initial part of the equilibrium adsorption isotherm in experiments at feed partial pressures lower than 4 kPa.

APPENDIX

The well-known methods to check for mass transfer limitation are based on the kinetics of irreversible steady-state reactions (30). However, these methods cannot be applied to situations where concentrations change with time; for example, during breakthrough of an adsorbable component in a packed bed adsorber. Anderson (31) derived a criterion for isothermal behavior of catalyst pellets during reaction. We followed his line of reasoning to express the actual uptake of an isothermal, spherical particle in terms of observables.

The present paper describes measurements of breakthrough curves using binary mixtures with one adsorbable component (carbon dioxide). Stable breakthrough curves with large linear parts result because of its favorable isotherm. As the mass transfer resistance in the macropores is limiting, the amounts adsorbed are in equilibrium with the local macropore concentrations, and the amount adsorbed at the particle surface is in equilibrium with the bulk of the gas phase. At the linear part of the breakthrough curve and after an initial time, the limiting solution of a constant flux problem has to emerge. The quantities adsorbed locally in the particle will then all increase at the same speed, and a stable but rising concentration profile results, see Fig. A1, so $\partial \bar{q}/\partial t \approx \partial q_R/\partial t$, where $\bar{q}$ is the average uptake and q_R is the uptake at the particle surface. The stable profile only offers a valid limitation investigation test method if the time needed to reach such a profile is short compared to the span of time in which breakthrough occurs.

Evaluation of the limitation investigation tool should take place at the steepest (linear) part of the breakthrough curve, where limitation is most likely. To compare the relative importance of the limitation between experiments, a point of reference has to be chosen. We chose to evaluate the test method at the point where the mole fraction is half the feed mole fraction.

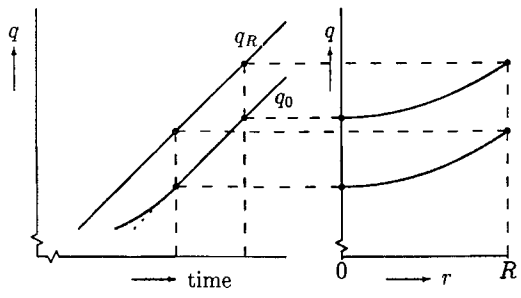

FIG. A1 Relation between the uptake in time (left) and the adsorption profiles as a function of the radius in a particle (right).

For small deviations from q_R, the adsorption isotherm may be linearized around q_R:

$$q_r = q_R - (y_R - y_r)\frac{dq_R}{dy} \tag{A1}$$

To enhance readability we define $q_r = q(r, t)$ and $y_r = y(r, t)$ as, respectively, the amount adsorbed locally and the macropore gas phase mole fraction at radius r, so q_r and y_r are in equilibrium.

Second, a reasonable description of the concentration profile is (32, 33)

$$y_r = y_R - (y_R - y_0)\left(1 - \frac{r^2}{R^2}\right) \tag{A2}$$

where y_0 is the mole fraction in the center of the particle. y_0 follows from the mass balance over an entire particle:

$$\frac{4}{3}\pi R^3 \rho_s \frac{\partial \bar{q}}{\partial t} = 4\pi R^2 D_{eff} c \left.\frac{\partial y}{\partial r}\right|_{r=R} = 8\pi R D_{eff} c (y_R - y_0) \tag{A3}$$

where, by definition:

$$\bar{q} = \frac{\int_0^R 4\pi r^2 q_r dr}{\frac{4}{3}\pi R^3} \tag{A4}$$

Finally, after eliminating q_r, y_r, and y_0 from Eqs. (A1)–(A4), and noting that $\partial \bar{q}/\partial t \approx dq_R/dy_R \cdot \partial y_R/\partial t$, integration of Eq. (A4) leads to

$$\frac{\Delta q}{q_R} = \frac{q_R - \bar{q}}{q_R} = \frac{\rho_s R^2}{15 q_R \mathbf{D}_{eff} c} \left(\frac{dq_R}{dy}\right)^2 \frac{\partial y_R}{\partial t} \qquad \text{(A5)}$$

This relation, in which the isotherm equation is not yet specified, expresses the influence of mass transfer limitation on the uptake of an isothermal spherical particle with radius R in terms of observables: the slope of the breakthrough curve $\partial y_R/\partial t$, the slope of the isotherm dq_R/dy at the gas phase concentration y_R and the uptake q_R, which is also calculated from the isotherm at y_R.

Equation (A5) shows that for experiments with a steeper breakthrough curve, mass transfer limitation is more important. The equation also indicates that at high concentrations, where the slope of the isotherm approaches zero, the influence of mass transfer limitation on the uptake becomes negligible.

ACKNOWLEDGMENTS

The volumetric adsorption isotherm measurements by Dr. R. de Lange (University of Twente) and Mr. J. Loos (University of Delft), and the effective diffusivity measurements by Mr. F. Reijnen are gratefully acknowledged.

SYMBOLS

A	cross-sectional column area (m^2)
B	Langmuir adsorption constant (Pa^{-1})
C_p	heat capacity of the gas [J/(kg·K)]
d	particle diameter (m)
$\mathbf{D}$	dispersion coefficient (m^2/s)
$\mathbf{D}_{eff}$	effective diffusion coefficient in a pellet (m^2/s)
k	constant in Eq. (1) (Pa·s/mol)
L	length of the column (m)
p	total pressure (Pa)
P	dimensionless total pressure p/p_∞ (—)
Pe_m	Péclet number $Lu_\infty/\mathbf{D}$ (—)
Pe_{hp}	Péclet number for heat transfer based on the particle diameter $u_\infty \rho_g C_p d/\lambda_g$ (—)
q	quantity adsorbed (mol/kg)
q_{mono}	monolayer uptake (mol/kg)
Q	dimensionless quantity adsorbed $\rho_s qRT/p_\infty$ (—)

R	gas constant [J/(mol·K)]
	Appendix: particle radius (m)
$\mathcal{R}$	rate of adsorption $\rho_b \partial q/\partial t$ [mol/(m^{3}s)]
t	time (s)
T	temperature (K)
u	interstitial velocity (m/s)
U	dimensionless interstitial velocity u/u_∞ (—)
W	quantity of adsorbent (kg)
x	distance (m)
y	mole fraction (of the adsorbing component) (—)
z	dimensionless distance x/L (—)

Greek Letters

ϵ	interstitial porosity of the bed (—)
ϵ_t	total porosity of the bed (—)
λ_g	heat conductivity of the gas phase [J/(s·m·K)]
ϕ	total molar (feed) flow (mol/s)
ρ_b	bed density of the adsorbent $(1 - \epsilon)\rho_s$ (kg/m^3)
ρ_g	gas phase density (kg/m^3)
ρ_s	adsorbent density (kg/m^3)
τ	dimensionless time tu_∞/L (—)

Subscripts

e	at the exit of the column
f	feed
i	component number
∞	final value

REFERENCES

1. R. Yang and S. Doong, "Gas Separation by Pressure Swing Adsorption: A Pore-Diffusion Model for Bulk Separation," *AIChE J.*, *31*, 1829–1842 (1985).
2. K. Chihara and M. Suzuki, "Simulation of Nonisothermal Pressure Swing Adsorption," *J. Chem. Eng. Jpn.*, *16*, 53–61 (1983).
3. J. Carter and M. Wyszynski, "The Pressure Swing Adsorption Drying of Compressed Air," *Chem. Eng. Sci.*, *38*, 1083–1099 (1983).
4. R. Yang, S. Doong, and P. Cen, "Bulk Gas Separation of Binary and Ternary Mixtures by Pressure Swing Adsorption," *AIChE Symp. Ser.*, *81*, 84–94 (1985).
5. L. Shendelman and J. Mitchell, "A Study of Heatless Adsorption in the Model System CO_2 in He, I," *Chem. Eng. Sci.*, *27*, 1449 (1972).
6. Y. Chan, F. Hill, and Y. Wong, "Equilibrium Theory of a Pressure Swing Adsorption Process," *Ibid.*, *36*, 243–251 (1981).
7. K. Knaebel and F. Hill, "Pressure Swing Adsorption: Development of an Equilibrium Theory for Gas Separations," *Ibid.*, *40*, 2351–2360 (1985).

8. S. Nataraj and P. Wankat, "Multicomponent Pressure Swing Adsorption (MCPSA)," *AIChE Symp. Ser.*, *78*, 29–38 (1982).
9. G. Flores Fernandez and C. Kenney, "Modelling of the Pressure Swing Air Separation Process," *Chem. Eng. Sci.*, *38*, 827–834 (1983).
10. S. Doong and R. Yang, "Bulk Separation of Multicomponent Gas Mixtures by Pressure Swing Adsorption: Pore/Surface Diffusion and Equilibrium Models," *AIChE J.*, *32*, 397–410 (1986).
11. R. Underwood, "A Model of a Pressure Swing Adsorption Process for Nonlinear Adsorption Equilibrium," *Chem. Eng. Sci.*, *41*, 409–411 (1986).
12. X. Lu, R. Madey, D. Rothstein, M. Jaroniec, and J.-C. Huang, "Pressure Swing Adsorption for a System with a Langmuir–Freundlich Isotherm," *Ibid.*, *45*, 1097–1103 (1990).
13. A. Bossy, D. Tondeur, and A. Jedrzejak, "A Nonlinear Equilibrium Analysis of Blowdown Policy in Pressure-Swing-Adsorption Separation," *Chem. Eng. J.*, *48*, 173–182 (1992).
14. S.-S. Suh and P. Wankat, "A New Pressure Swing Adsorption Process for High Enrichment and Recovery," *Chem. Eng. Sci.*, *44*, 567–574 (1989).
15. J. Kayser and K. Knaebel, "Pressure Swing Adsorption: Development of an Equilibrium Theory for Binary Gas Mixtures with Nonlinear Isotherms," *Ibid.*, *44*, 1–8 (1989).
16. M. LeVan and T. Vermeulen, "Channeling and Bed-Diameter Effects in Fixed-Bed Adsorber Performance," *AIChE Symp. Ser.*, *80*, 34–43 (1984).
17. F. Foeth, M. Andersson, H. Bosch, G. Aly, and T. Reith, "Separation of Dilute CO_2–CH_4 Mixtures by Adsorption on Activated Carbon," *Sep. Sci. Technol.*, *29*, 93–118 (1994).
18. G. Baron, H. Verelst, and R. Konduru, "Modeling and Optimal Control of Pressure Swing Parametric Pumping Air Separation," in *ESC 2*, VNU Science Press, Antwerp, 1986, pp. 520–526.
19. J. Kayser and K. Knaebel, "Integrated Steps in Pressure Swing Adsorption Cycles," *Chem. Eng. Sci.*, *43*, 3015–3022 (1988).
20. R. Kumar, "Adsorption Column Blowdown: Adiabatic Equilibrium Model for Bulk Binary Gas Mixtures," *Ind. Eng. Chem. Res.*, *28*, 1677–1683 (1989).
21. C.-T. Chou and W.-C. Huang, "Incorporation of a Valve Equation into the Simulation of a Pressure Swing Adsorption Process," *Chem. Eng. Sci.*, *49*, 75–84 (1993).
22. J. Kärger and D. Ruthven, *Diffusion in Zeolites and Other Microporous Solids*, Wiley, New York, 1992.
23. E. Wicke, "Bedeutung der molekularen Diffusion für chromatographische Verfahren," *Ber. Bunsenges.*, *77*, 160–171 (1973).
24. G. Langer, A. Roethe, K.-P. Roethe, and D. Gelbin, "Heat and Mass Transfer in Packed Beds—III: Axial Mass Dispersion," *Int. J. Heat Mass Transfer*, *21*, 751–759 (1978).
25. R. Bird, W. Stewart, and E. Lightfoot, *Transport Phenomena*, Wiley, New York, 1960.
26. W. Schiesser, *The Numerical Method of Lines: Integration of Partial Differential Equations*, Academic Press, San Diego, 1991.
27. A. Hindmarsh, "ODEPACK, A Systematized Collection of ODE Solvers," in *IMACS Transactions on Scientific Computation*, Vol. 1 (R. Stepleman, Ed.), North-Holland Publishing Co., Amsterdam, 1983, pp. 55–64.
28. R. Yang, *Gas Separation by Adsorption Processes* (Butterworths Series in Chemical Engineering), Butterworths, Boston, 1987.
29. E. Tsotsas, "Transportvorgänge in Festbetten: Geschichte, Stand und Perspektiven der Forschung," *Chem.-Ing.-Tech.*, *64*, 313–322 (1992).

30. D. Mears, "Tests for Transport Limitations in Experimental Catalytic Reactors," *Ind. Eng. Chem., Process Des. Dev., 10*, 541–547 (1971).
31. J. Anderson, "A Criterion for Isothermal Behaviour of a Catalyst Pellet," *Chem. Eng. Sci., 18*, 147–148 (1963).
32. C. Liaw, J. Wang, R. Greenkorn, and K. Chao, "Kinetics of Fixed Bed Adsorption: A New Solution," *AIChE J., 25*, 376 (1979).
33. M. Tsai, S. Wang, R. Yang, and N. Desai, "Temperature-Swing Separation of Hydrogen–Methane Mixture," *Ind. Eng. Chem., Process Des. Dev., 24*, 57 (1985).

Received by editor May 15, 1995